

Short Communication

Novel core-shell Structure TiO₂@TiN Spheres as High-Performance Anode Material for Lithium-Ion Battery

Wang Yinwei¹, Liu Shoufa^{2*}, Zhang Ning¹, Qiao Xun¹, Zhou Zhaofeng³

¹ Intelligent Manufacturing Research and Development Center, Xijing University, Xi'an 710123, China

² School of Mechanical Engineering, Xijing University, Xi'an 710123, China

³ College of Mechanical and Electrical Engineering, Nanjing University of Aeronautics and Astronautics, Nanjing 210016, China

*E-mail: shoufaliu2000@sina.com liushoufa@xijing.edu.cn

Tel: +86 15829479396

Received: 30 August 2018 / Accepted: 23 October 2018 / Published: 30 November 2018

Novel core-shell structure TiO₂@TiN spheres are successfully synthesized as anode materials for Li-ion batteries. The obtained TiO₂@TiN electrodes exhibit superior rate performance and perfect cycle performance. The capacity of TiO₂@TiN electrodes remain 286 mAh g⁻¹ after 200 cycles at 0.1 C. Even when the current density improves to 40 C, the capacity retention of TiO₂@TiN is about 89% after 300 cycles. This improved electrochemical performance of TiO₂@TiN is ascribed to the presence of TiN, which could enhance the conductivity and suppress the aggregation of TiO₂ at the same time.

Keywords: Energy storage and conversion; TiO₂@TiN spheres; Li-ion battery; Nanoparticles.

1. INTRODUCTION

During the past decades, anatase TiO₂ have drawn much attention of the researchers due to their promising application as anode materials in lithium-ion batteries [1, 2, 3]. This is because the anatase TiO₂ possesses following advantages, such as its high specific capacity, low cost and environmentally friendliness. However, in the process of the employment of TiO₂, some problems still limit its commercialization [4, 5, 6]. This is mainly attributed to the poor electronic conductivity and the aggregation of TiO₂ during the electrochemical process [7, 8].

Therefore, to improve the electrochemical performance of anatase TiO₂, the most efficient way is designing TiO₂-based composite material [9, 10]. Zhou et al prepared MoS₂ doped TiO₂ nanofibers composites via hydrothermal reaction. The as-prepared composites showed superior cycle stability for

100 cycles [11]. More recently, novel SnO₂/TiO₂ hybrid anode material was synthesized to guarantee the structural stability and excellent electrochemical properties [12]. From these works, it can be seen that the efficient method to improve the electrochemical performance of TiO₂ anode material is designing optimal TiO₂-based composite anode materials.

In this paper, inspired by these reports, novel structure of core-shell TiO₂@TiN composite was firstly prepared as anode materials for lithium-ion batteries. The TiN shell layer on the TiO₂ sphere could enhance the conductivity and suppress the aggregation of TiO₂ at the same time. As a result, the as-prepared core-shell TiO₂@TiN composites exhibit excellent electrochemical performance.

2. EXPERIMENT

2.1. Preparation of TiO₂@TiN composite

Firstly, 50 ml KCl solution (0.2 M) was prepared and kept static for 30 min. After that, 3.5 g HDA was added into the solution under uniform stirring. Then, 10 ml TIP was dropped into this mixture for 30 min. Finally, the solution mixed with 1.0 ml ammonia were transferred into stainless steel reactor at 180°C for 16h. The resultant TiO₂ spheres were washed by ethanol for three times. To prepare TiO₂@TiN composites, the as-prepared TiO₂ spheres were further annealed at 700°C for 1 h under NH₃ atmosphere. As a result, the core-shell TiO₂@TiN composites were obtained.

2.2. Material Characterization

The morphology and crystal structure information were obtained Transmission electron microscope (JEM-2010HR) and XRD (D8 Advance, Cu K α radiation).

2.3. Electrochemical Measurements

The electrochemical performance of TiO₂@TiN composite electrode was evaluated using a CR2016-type coin battery, which were assembled by using TiO₂@TiN as working electrode, Li metal as the counter electrode in an argon filled glove box. A solution of 1.0 M LiPF₆ was dissolved in 1:1 (v/v) EC/DEC as the electrolyte. The cycle performance test was conducted in the voltage range of 1.0-3.0 V on LAND battery tester. Electrochemical impedance spectra (EIS) measurement was carried out on an electrochemistry workstation (CHI660E).

3. RESULTS AND DISCUSSION

Figure 1 shows the whole preparation process of core-shell TiO₂@TiN composite. TiO₂ spheres were firstly prepared via hydrothermal reaction method. After that, TiO₂@TiN composites were synthesized via forming TiN layer on the surface of TiO₂ spheres. The XRD pattern of TiO₂@TiN exhibits the sharp diffraction peaks, indicating good crystallization of the products (Figure 2).

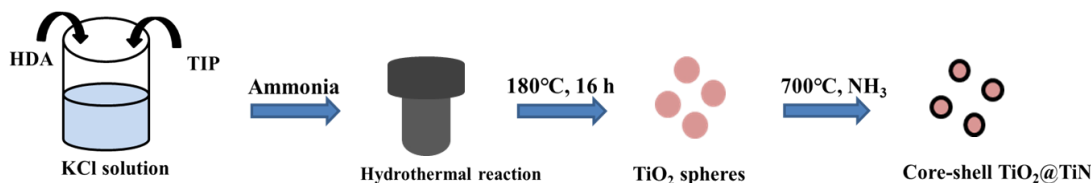


Figure 1. The graphical illustration of the formation process for the core-shell TiO₂@TiN composite.

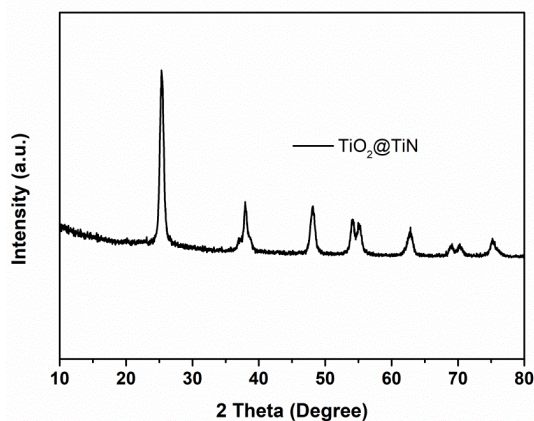


Figure 2. The XRD pattern of TiO₂@TiN composite.

Figure 3 shows the TEM image of as-prepared TiO₂@TiN composite. It can be seen that the TiO₂@TiN composite exhibits core-shell structure. The TiO₂ sphere core is surrounded by the TiN shell layer. The diameter of all core-shell TiO₂@TiN sphere composites is in the range of 80-100 nm. To confirm the uniform distribution of the elements, the corresponding elemental mapping of Ti, O, N was conducted. As shown in Fig. 2 b-d, Ti, O, N elements are uniformly dispersed in the TiO₂@TiN composite. The selected area electron diffraction pattern of TiO₂@TiN composite is shown in Fig. S1. It further indicates the presence of anatase TiO₂ and TiN.

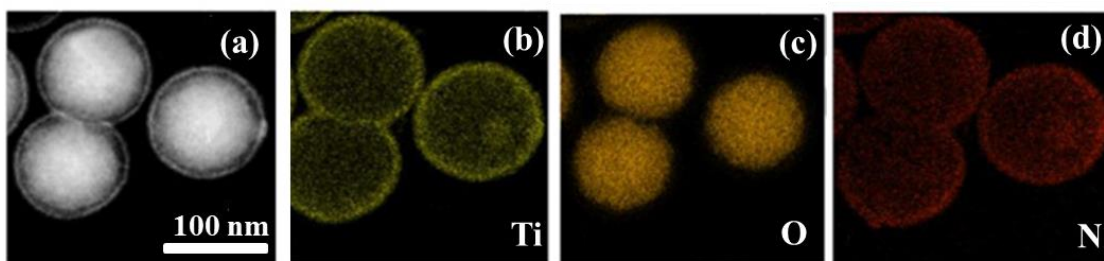


Figure 3. (a) TEM image of TiO₂@TiN composite. Corresponding elemental mapping of (b) Ti, (c) O and (d) N.

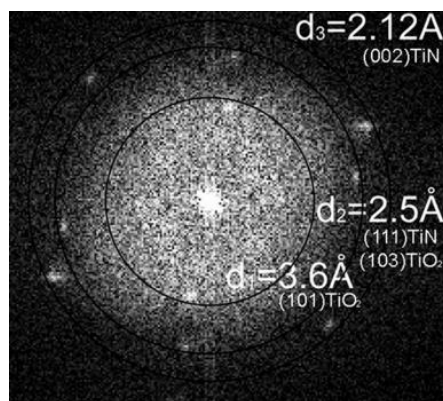


Figure 4. The selected area electron diffraction pattern of $\text{TiO}_2@\text{TiN}$ composite.

Figure 5 a is the initial discharge-charge profiles of $\text{TiO}_2@\text{TiN}$ composite electrode at 0.1 C. There are two voltage platforms at 2.0 V and 1.7 V, respectively, corresponding the charge platform and discharge platform [13]. Moreover, the first specific discharge capacity of $\text{TiO}_2@\text{TiN}$ composite electrode is as high as 326 mAh g^{-1} . Figure 4 b shows the cycle performances of pure TiO_2 and $\text{TiO}_2@\text{TiN}$ electrode at 0.1 C. It can be seen that the capacity of $\text{TiO}_2@\text{TiN}$ composite electrode remains at 256 mAh g^{-1} after 200 cycles. While the pure TiO_2 electrode only exhibits specific capacity of 158 mAh g^{-1} . This indicates that the core-shell $\text{TiO}_2@\text{TiN}$ composite electrode possesses more excellent cycle stability than pure TiO_2 electrode [14].

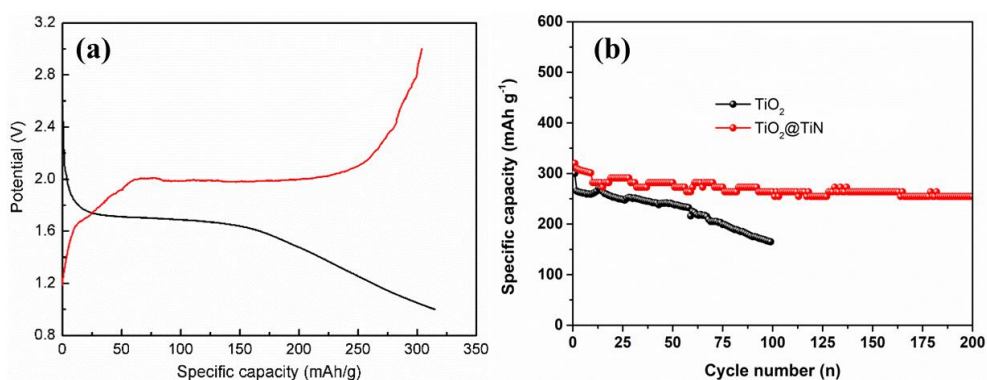


Figure 5. (a) The initial discharge-charge profiles of $\text{TiO}_2@\text{TiN}$ composite electrode at 0.1 C. (b) The cycle performances of pure TiO_2 and $\text{TiO}_2@\text{TiN}$ composite electrode.

As shown in Figure 6, the electrochemical impedance spectra of both sample electrodes are consisted of two parts: semicircle in the high frequency area and slant line in the low frequency area. The semicircle represents contact impedance between the electrolyte and the electrode material and the charge transfer resistance. The slant line represents Warburg impedance [15]. It can be seen from the figure that $\text{TiO}_2@\text{TiN}$ composite displays smaller charge transfer resistance than pure TiO_2 electrode, which demonstrates that more superior electronic conductivity.

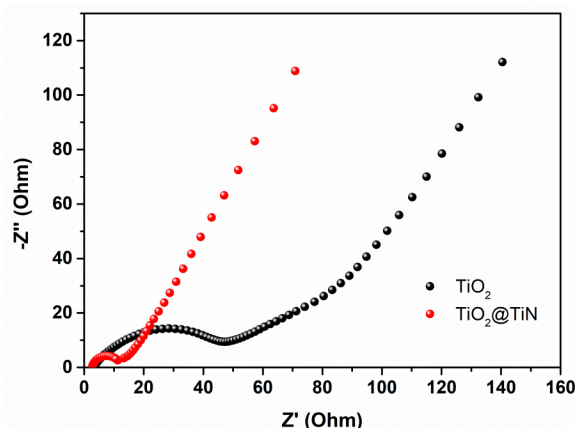


Figure 6. EIS of pure TiO₂ and TiO₂@TiN composite electrode.

To further demonstrate the superior performance of TiO₂@TiN, long-term cycle performance was tested at the current density of 40 C. As shown in Figure 7, a high specific capacity value of 215 mAh g⁻¹ was achieved for the TiO₂@TiN composite electrodes after 300 cycles. This excellent cycle performance is ascribed to the presence of TiN in the TiO₂@TiN composite, which could improve the electronic conductivity and suppress the aggregation of TiO₂ at the same time.

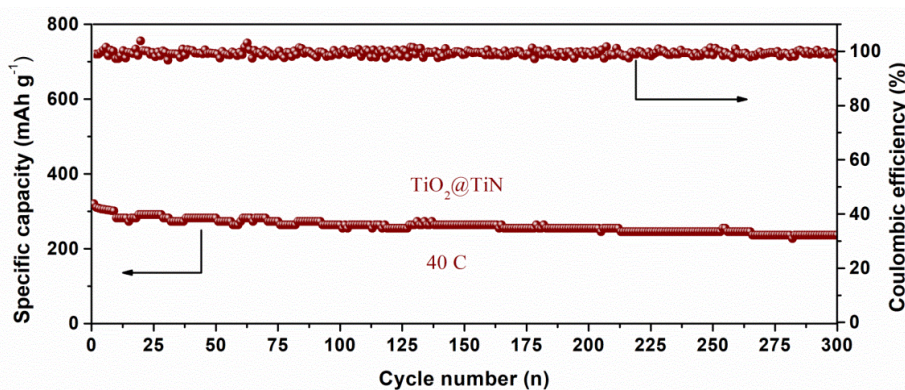


Figure 7. Long-term cycle performance of TiO₂@TiN composite electrode at 40 C.

The rate performances of pure TiO₂ and TiO₂@TiN composite were tested at various current densities from 0.05 C to 20 C. As shown in Figure 8, it can be seen that the specific capacity of TiO₂@TiN composite electrode was 368 mAh g⁻¹ at 0.05 C. When the current densities were improved to 1 C, 5 C and 10 C, the specific capacities of TiO₂@TiN composite electrode were still remain at high values. Even the capacity value of TiO₂@TiN composite electrode was 286 mAh g⁻¹ at the high current density of 20 C. However, in terms of the pure TiO₂ electrode, its capacity value faded rapidly when the current densities were improved from 0.05 C to 20 C. Besides, when the current density was returned to 1 C, the capacity value of TiO₂@TiN composite electrode could recover back. The pure TiO₂ electrode could not endure various current densities.

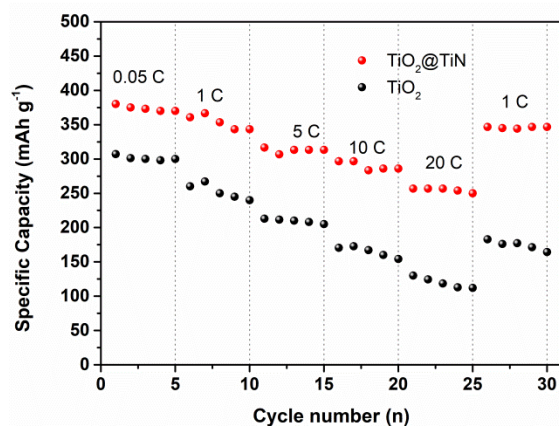


Figure 8. The rate performances of pure TiO_2 and $\text{TiO}_2@\text{TiN}$ composite electrode.

As shown in Table 1, we made a comparison of various anode materials for Li-ion batteries. It can be clearly observed that the as-prepared $\text{TiO}_2@\text{TiN}$ composites electrode showed more excellent cycle stability than other materials reported in the literature. This result also proved that the $\text{TiO}_2@\text{TiN}$ composites were promising anode materials for the Li-ion batteries.

Table 1. The comparison of various anode materials for Li-ion batteries.

Samples	Current Density	Capacity (Cycle number)	Reference
$\text{TiO}_2@\text{TiN}$	40 C	215 (300)	This work
TiO_2	20 C	208 (150)	[16]
ETO	40 C	192 (100)	[17]

4. CONCLUSIONS

In summary, core-shell structure of $\text{TiO}_2@\text{TiN}$ composite was firstly prepared and used as anode materials for Li-S batteries. The $\text{TiO}_2@\text{TiN}$ composite electrodes deliver a high initial capacity of 325 mAh g^{-1} and maintain 286 mAh g^{-1} after 200 cycles at 0.1 C. Even at 40 C, the $\text{TiO}_2@\text{TiN}$ composite electrodes exhibit excellent capacity retention of 89% after 300 cycles.

ACKNOWLEDGEMENT

This research is financially supported by National Key S&T Special Projects (2017ZX04011010), and Research project of Shaanxi Provincial Education Department (15JK2172).

References

1. Q. H. Tian, J. B. Yan and L. Yang, *Electrochim. Acta* 282 (2018) 38.
2. H. M. Zhou, P. F. Lv and X. Xia, *Mater. Lett.* 218 (2018) 47.
3. R. Premila, C. Subbu and S. Rajendra, *Appl. Surf. Sci* 449 (2018) 426.

4. H. Huang, J. G. Yu and Y. P. Gan, *Mater. Res. Bull.* 96 (2017) 425.
5. L. Gao, L. C. Wang and S. Dai, *J. Power Sources* 344 (2017) 223.
6. S. Zhu, K. Chu and H. Sakuyama, *Electrochim. Acta* 212 (2016) 481.
7. Z. Y. Li, F. X. Ding and Y. G. Zhao, *Ceram. Int.* 42 (2016) 15464.
8. S. H. Moon, S. J. Kim and M. C. Kim, *J. Alloy Comput.* 741 (2018) 1048.
9. C. Y. Zhao, L. J. Liu and Q. Y. Zhang, *Electrochim. Acta* 155 (2015) 288.
10. W. Wen, J. M. Wu and Y. Z. Jiang, *Chem 2* (2017) 404.
11. H. M. Zhou, P. F. Lv, X. Xia, J. Zhang, J. Yu, Z. Y. Pang, H. Qiao and Q. F. Wei, *Mater. Lett.*, 218 (2018) 47.
12. X. H. Zhu, S. S. Jan, F. Zan, Y. D. Wang and H. Xia, *Mater. Res. Bull.*, 96 (2017) 405.
13. H. M. Shi, H. Zhang and Z. Chen, *Chem. Eng. J.* 336 (2018) 12.
14. Z. M. Wang, Y. Cheng and Q. Li, *J. Power Sources* 389 (2018) 214.
15. C. Li, M. Zhao and C. N. Sun, *J. Power Sources* 397 (2018) 162.
16. J. Q. Guo, J. Li, Y. J. Huang, M. Zeng and R. F. Peng, *Mater. Lett.*, 181 (2016) 289.

© 2019 The Authors. Published by ESG (www.electrochemsci.org). This article is an open access article distributed under the terms and conditions of the Creative Commons Attribution license (<http://creativecommons.org/licenses/by/4.0/>).